ISSN No: 2348-4845
International Journal & Magazine of Engineering, Technology, Management and Research
A Peer Reviewed Open Access International Journal

Design and Implementation of Wireless and Wearable EEG System for Evaluating Driver Vigilance

Karthik C
Research Scholar,
Dept of ECE,
Pondicherry Engineering College,
Puducherry 605014.

Dr Swaminadan V
Professor,
Dept of ECE,
Pondicherry Engineering College,
Puducherry 605014.

Abstract:

Brain activity associated with attention sustained on the task of safe driving has received considerable attention recently in many neurophysiological studies. Those investigations have also accurately estimated shifts in drivers' levels of arousal, fatigue, and vigilance, as evidenced by variations in their task performance, by evaluating electroencephalographic (EEG) changes. However, monitoring the neurophysiological activities of automobile drivers poses a major measurement challenge when using a laboratory-oriented biosensor technology.

This work presents a novel dry EEG sensor based mobile wireless EEG system (referred to herein as Mindo) to monitor in real time a driver's vigilance status in order to link the fluctuation of driving performance with changes in brain activities. The proposed Mindo system incorporates the use of a wireless and wearable EEG device to record EEG signals from hairy regions of the driver conveniently. Additionally, the proposed system can process EEG recordings and translate them into the vigilance level. The study compares the system performance between different regression models.

Moreover, the proposed system is implemented using JAVA programming language as a mobile application for online analysis. A case study involving 15 study participants assigned a 90 min sustained-attention driving task in an immersive virtual driving environment demonstrates the reliability of the proposed system.

Consistent with previous studies, power spectral analysis results confirm that the EEG activities correlate well with the variations in vigilance. Furthermore, the proposed system demonstrated the feasibility of predicting the driver's vigilance in real time.

Introduction

Drowsiness significantly contributes to automobile accidents leading to a considerable number of traffic collisions, injures fatalities annually [1]. Developing an effective system for detecting drowsiness is thus of priority concern for real-life driving. Such an in-vehicle system must continuously monitor the arousal status of drivers and accurately predict the potential impact on behavioral lapse. Several bio-behavioral signatures have been developed to monitor drowsiness of automobile drivers, including eye blinking [2] and head nodding [3]. However, false alarms are likely since these visual attributes are not always accompanied by drowsiness [4].

Related studies in recent decades have demonstrated that electroencephalography (EEG), i.e., the electric fields produced by brain activity, is a highly effective physiological indicator for assessing vigilance states [5]–[8]. EEG is the only brain imaging modality with a high temporal and fine spatial resolution that is sufficiently lightweight to be worn in operational settings [9]. Numerous EEG studies suggest that delta (1–3 Hz), theta (4–7 Hz), and alpha (8–12 Hz) activities are highly correlated with fatigue, drowsiness, and poor task performance [10]–[12].

ISSN No: 2348-4845
International Journal & Magazine of Engineering, Technology, Management and Research
A Peer Reviewed Open Access International Journal

By using the conventional wet and wire EEG acquisition system (i.e., Neuroscan System), our previous studies [13]–[17] explored driver brain activity changes: from alertness to drowsiness. Based on the neurological findings, drowsiness monitoring algorithms were developed by using several machine learning methods. The experimental results further demonstrated the feasibility of detecting or monitoring driver drowsiness level using EEG signals.

However, designing a user acceptable and feasible EEG device to realize the real-time monitoring system is still a challenging task. Data collection in most EEG studies requires skin preparation and conductive gel application to ensure excellent electrical conductivity between a sensor and human skin. These procedures are time consuming, uncomfortable, and even painful for participants [18], [19].

Additionally, the signal quality may degrade over time as the conductive gel dries out [20]. Hence, a wearable and wireless dry- electrode EEG system must be developed, capable of assessing the brain activities of participants performing ordinary tasks. According to a previous study [15], spectral dynamics of EEG at posterior brain regions are strongly correlated with the deterioration of task performance and declining vigilance.

In [13], the power spectra were successfully linked with behavioral performance by regression models. Additionally, the advantage of using the EEG signals of the posterior brain region has been shown in a recent study [17] that the classification performance of the drowsiness detection system using the EEG signals of parietal and occipital regions is significantly better than that

TABLE I
COMPARISON OF DRY EEG SYSTEMS

Dry EEG system	Mindo-4	Cognionics [53]	Enobio [54]	NeuroSky [23]	DSI 10/20 [55]	imec [56]
Sensor Type	Dry	Dry and active	Dry	Dry	Dry	Dry and active
Bandwidth	0.23 – 125 Hz	0-50Hz	0 - 50Hz	3 - 100Hz	0.02-120Hz	0.5-100Hz
Resolution	24bits	24bits	24bits	12bits	16bits	12bits
#(Channels)	4	16/24/32/ 64	8/20	1	23	8
Sampling rate	128/256/512 Hz	300Hz	500 Hz	512Hz	240/960Hz	1024Hz
Transfer	wireless	wireless	wireless	wireless	wireless	wireless
Weight	100g	350g	65g	90g	500g	N/A
Battery life (hour)	23	6	16	8	24	22-70
Signal quality compared with conventional wet EEG systems	Correlation coefficient: >92% [29]	Correlation coefficient: >90% [57]	No significant difference [58]	Correlation coefficient: >70% [59]	Correlation coefficient: >80% [60]	Correlation coefficient: 81%-98% [56]

Using the EEG signals of the frontal region. However, these studies [13], [15], [17] still used conventional wet EEG electrodes in measuring EEG signals. Hence, acquiring the EEG signal of the hair region is a critical factor in developing a successful vigilance monitoring system. Recent studies have measured EEG signals using dry sensors, including silicone conductive rubber [21], comb-like electrode [22], goldplated electrode [23], bristle -type electrode [24], and foam-based sensor [25]. Table I lists some commercially available EEG systems. Most of these dry sensors are useful for hairy sites. EEG acquisition from the posterior region is available.

This study develops an EEG-based in-vehicle system for assessing human vigilance level. EEG dynamics and behavioral changes of participants are simultaneously recorded via a new dry-contact EEG device [26], [27] with spring-loaded sensors [28], [29] when they perform a sustained-attention driving task. Additionally, an effective system using support vector regression (SVR) [30] is developed to model the relationship between the brain activity and the behavioral performance. The system performance of SVR-based model is compared with other state-of-art regression methods. Moreover, the prediction model is implemented on a portable device.

ISSN No: 2348-4845
International Journal & Magazine of Engineering, Technology, Management and Research
A Peer Reviewed Open Access International Journal

Furthermore, feasibility of the pro-posed system is demonstrated by monitoring human cognitive states during a sustained-attention driving task [31].

II. SYSTEM ARCHITECTURE

Fig. 1 shows the proposed EEG-based in-vehicle system, de-signed to monitor human vigilance level continuously during automobile driving. To construct the system, EEG signals were recorded using a mobile and wireless EEG device with dry sensors when the participants performed a sustained-attention task in a realistic dynamic driving simulator [32]. For data acquisition, the wireless and mobile EEG system, as shown in Fig. 2, consists of dry electrodes, data acquisition module, Bluetooth transition module, and rechargeable battery. The device was de-signed for quickly and conveniently recording an EEG signal of the occipital region which is highly correlated with the vigilance [15]. This dry EEG system surpasses the conventional wet electrodes with the conduction gel for long- term EEG measurements [25].

Additionally, the signal quality of the used dry EEG system is comparable with that of the NeuroScan [29]. For data analysis, the pre-stimulus EEG spectra of all experimental trials were segmented and formed as a training dataset of samples after applying band-pass filter (0.5–50 Hz) and fast Fourier transformation (FFT) [33]. Each training sample was ac-companied with the behavioral performance in response to the given task, indicating the presumable vigilance of a driver. As for the core of the prediction system, the relationship between EEG and behavior was modelled using support vector regression (SVR) [30]. Finally, the predicted outputs were converted to different levels of vigilance. For real - world applications, the proposed system was implemented on a mobile device using JAVA programming language. The wireless and wearable EEG device transmitted its recorded data via a Bluetooth interface to the user's device. The acquired EEG is displayed, processed, and analyzed in real time. The following sections introduce in detail the major components of the proposed system.

A. Dry EEG Electrodes

As shown in Fig. 2(a)–(c), a new dry-contact EEG device with spring-loaded sensors [28] was proposed for potential operations in the presence or absence of hair and without any skin

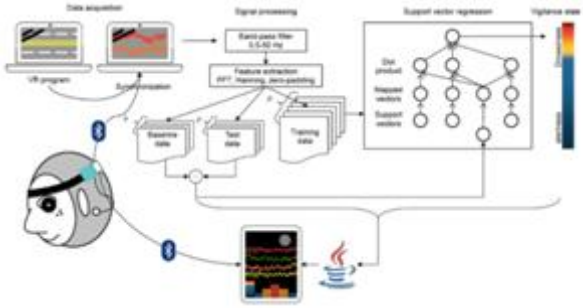

Fig. 1. Design of EEG signal acquisition, processing, and analysis system, where, and denote the number of training samples, lags, and baseline samples, respectively. The real-time vigilance monitoring system is implemented in a tablet-based application using Java programming language.

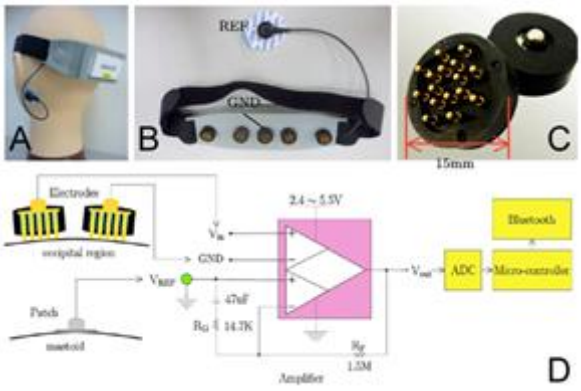

Fig. 2. Wireless and wearable EEG devices. (a) Wireless and wearable EEG headsets. (b) Five dry EEG electrodes and one patch sensor. (c) Spring-loaded probes. (d) Block diagram of the circuit.

Preparation or conductive gel usage. Each probe was designed to include a probe head, plunger, spring, and barrel. The 17 probes were inserted into a flexible substrate using a one-time forming process via an established injection molding procedure. With 17 spring contact probes, the flexible substrate allows for a high geometrical conformity between the sensor and the irregular scalp surface to maintain low skin-sensor interface impedance.

ISSN No: 2348-4845
International Journal & Magazine of Engineering, Technology, Management and Research
A Peer Reviewed Open Access International Journal

Additionally, the flexible substrate also initiates a sensor buffer effect, thereby eliminating pain when force is applied. This sensor is more convenient than conventional wet electrodes in measuring EEG signals without any skin preparation or conductive gel usage.

B. EEG Signal Acquisition Circuit

According to Fig. 2(d), the EEG acquisition module consists of four major components [28]: a amplifier (ISL28470, Intersil, USA);, a front-end analog -to-digital converter (ADC, AD1298, Analog Devices, USA), a microcontroller (MSP430, Texas Instruments, USA), and a wireless transmission (BM0403, Unigrand Ltd., Taiwan). The voltage between the electrode and the reference was amplified using a biosignal amplifier with high input impedance. Meanwhile, the common -mode noise was rejected to precisely detect microvolt-level brain wave signals from the scalp [34]. In particular, transfer function of the preamplifier, i.e., equivalent to the form of a high-pass filter with input signals of frequency , is as follows [35]: where, and in this study.

The gain of the preamplifier unit is set to 103 V/V the amplified signal was digitized via an ADC with a 24 bit resolution and 256 Hz sampling rate. The minimum input voltage of ADC ranges from to 1.94 mV. The maximum input voltage of ADC ranges from to 23.30 mV. In the microcontroller unit, the power-line interface was removed using a moving average filter with a frequency of 60 Hz. The digitalized signals after amplification and filtering were transmitted to a PC or a mobile device via Bluetooth with a baud-rate of 921600 bits/s. Power was supplied by a high capacity (750 mAh, 3.0 V) Li-ion battery, which provided 23 hr of continuous operation at maximum power consumption.

C. EEG Signal Processing and Analysis

During a 90 min driving experiment (see Section III), the study participants encountered hundreds of unexpected lane-departure events. In the signal processing, all 2 s baseline data (512 sampling points) before the stimuli were extracted from continuous EEG signals. The data in this baseline period, without any confounding factors (i.e., events, motion stimuli, and motor actions) were an appropriate segmentation of EEG signals to link the physiological message with the driving performance. The data pair of the-th trial is denoted as where 4 denotes the number of channels, represents the number of trials: ; and refers to the driving performance, as measured by the reaction time (RT) in response to the lane-departure event. First, a type I Chebyshev band-pass filter with cut-off frequencies of 0.5 Hz and 50 Hz was applied on the raw data to remove artifacts. Second, physiological features were extracted by transforming the EEG signals of all trials, into a frequency domain using FFT to characterize the spectral dynamics of brain activities. As shown in Fig. 4, the EEG signal was successively fed into a weighted time- frequency analysis before applying support vector regression. Power spectral density (PSD) of the EEG signal at time was the weighted average of power spectrum of previous

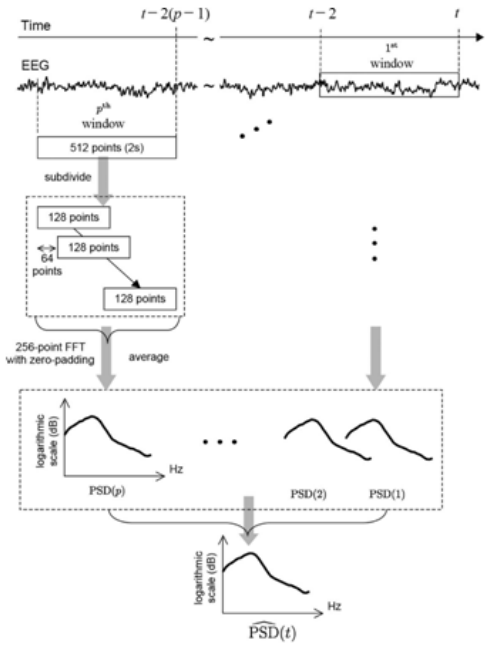

( )

Fig. 3. Spectral EEG feature extraction.

Power spectra at time, denoted by, are estimated by using FFT with Welch's method and a weighting scheme, where the spectral feature are extracted every

ISSN No: 2348-4845
International Journal & Magazine of Engineering, Technology, Management and Research
A Peer Reviewed Open Access International Journal

2 s. windows of EEG spectrum, in which all frequency responses of EEG activations were calculated using a 512-point moving window without overlapping points. Each 512 points (2 s) of data were further subdivided into several 128-point sub-windows advanced in a 64-point step. Windowed 128-point epochs were extended to 256 points by zero-padding in order to calculate the power spectra using a 256- point FFT (Welch's method), subsequently yielding an estimate of the power spectral density with 30 frequency bins from 1 to 30 Hz. The power spectra of these subwindows were converted into a logarithmic scale and averaged to form a log power spectrum for each window. Furthermore, the estimated spectral powers of four channels were averaged, and the mean power spectrum of the first 10 min of the experiment, which was putatively the alert pattern, was subtracted from each estimated spectrum. Since the periods of the cyclic fluctuations of drowsiness exceeded 4 min [36], variance at cycle lengths shorter than 1 min was eliminated using a weighted-averaging filter that advanced in a step of 2 s. Next, PSD of the window was multiplied by a weighted coefficient , where w decreased as increased. In this study, and compared with an unprocessed PSD without a weighted-averaging filter, a smoother PSD estimate is obtained by using this algorithm.

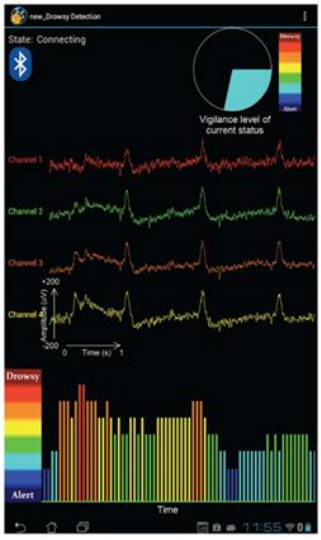

Fig. 4. Snapshot of the proposed driver drowsiness prediction system implemented on an Android platform.

The pie chart display the current level of driver's vigilance evaluated every 2 s. Four traces display the EEG recordings with refresh rate of five seconds. Color bars record the changes of vigilance level during driving.

D. Prediction Model

According to previous studies [15], the behavioral lapses induced by drowsiness correlate with the changes of EEG activities. To link the power spectra with RTs, a nonlinear model is preferred in the model fitting to cover linear and nonlinear relationships between EEG power spectra and RTs. The support vector machine is a conventional means of solving the multidimensional function estimation problem, and has been applied to various fields such as classification and regression. When used to solve the function approximation and regression estimation problems, SVM is denoted as the support vector regression (SVR)[30]. Fig. 1 shows the graphical framework of SVR, including the support vectors, mapped vectors, and dot product operations. SVR is a complex and heavy-computational implementation of a forecasting algorithm based on structuring risk minimization principles to obtain an effective generalization capability [37], [38].

The goal of -SVR is to find a small such that a function has at most deviationfrom for all the training data, where and denotes the dot product. According to [30], the -SVR, can be formulated as minimization of (3) and (4) as the following: where, are slack variables. The constant determines the compromise between the flatness of and the amount up to which deviations larger than are tolerated. In this study, the SVR model was implemented using a library of LIBSVM [39]. The dot product operation of any two mapped vectors can be implemented by a kernel function which satisfies Mercer's theorem [30]. In this study, most commonly used kernel functions, including linear, polynomial, radial basis function, and sigmoid function were implemented and their performances were com-pared. The formulas of these four kernels are listed as follows:

ISSN No: 2348-4845
International Journal & Magazine of Engineering, Technology, Management and Research
A Peer Reviewed Open Access International Journal

1) Linear kernel
2) Polynomial kernel
3) Radial basis function kernel (RBF kernel)
4) Sigmoid kernel

where determines the width of RBF function, is a constant trading off the higher-order versus lower-order term in the polynomial, is a scaling parameter of the input data, and is a shifting parameter controlling the threshold of mapping. The root mean square error (RMSE) is a conventional index for evaluating the performance of the predictor [40]. RMSE can be estimated as follows: (5) where RT and denote the observed reaction times and the predicted reaction times, respectively; and represents the number of validation datasets. A smaller RMSE implies a more accurate prediction for the used model.

E. Mobile Application

After yielding the optimal parameters of SVR, the proposed prediction model was incorporated in a mobile application using JAVA programming language to run on smartphones, tablet computers, and other mobile devices. This application connects wirelessly with a wearable EEG device via Bluetooth to record the subjects' EEG signal and evaluate their vigilance level directly. Fig. 4 displays the graphic user interface (GUI) of the developed mobile application. The raw EEG recordings of 4 channels displayed in the middle of GUI refresh every 5 s. The estimated vigilance level displaying in the upper right hand corner (circle icon) refreshes every 2 s.

The vertical bars shown in the bottom of GUI show the changes of vigilance level. The predicted RT was then converted into the presumable vigilance level byn (6) where rounding denotes the operator to return the value to the nearest integer, and represents the predicted RT. In this study, is set to 3. A "three-second" rule is generally recommended for the driver to follow in order to maintain a safe distance from the lead vehicle on the highway [41]. Here, parameter is set to 8, i.e., the total number of vigilance levels.

III. EXPERIMENTAL DESIGN AND MATERIALS

A. Subjects

Fifteen subjects participated in a sustained-attention driving task. Each subject wore a wireless and wearable EEG headset, sat inside the vehicle, and controlled the simulator by using the steering wheel. To easily induce drowsiness, the experiment began in the early afternoon (13:00–14:00) after lunch and lasted for approximately 90 min when the circadian rhythm of sleepiness reached its peak [42].

B. Driving Simulator

As shown in Fig. 5(a), the synchronized scenes were projected from six projectors to constitute a surrounding 360 vision. At the center of the projected scenes, a real vehicle (without the unnecessary weight of an engine and other components) was mounted on a six degree-of - freedom motion platform. The motion sensation was then delivered along with the movement of the vehicle. A four-lane highway scene projected on a surrounding screen simulates a visually monotonous and unexciting stimulus of a driving condition to induce drowsiness.

Additionally, the refresh rate of the highway scene was set properly to emulate a car driving at a fixed speed of 100 km/hr. The four lanes from left to right were separated by a median stripe. The distance from the left side to the right side of the road was equally divided into 240 units (digitized into values of 1–240): the widths of each lane and the car were 60 units and 28 units, respectively. These units were converted into the same ratio of the width of the real lane (3.75 m) and the car (1.8 m).

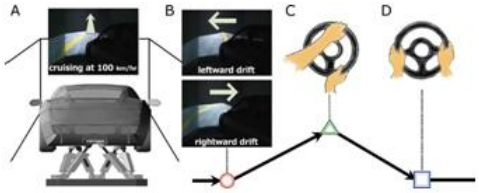

Fig. 5. Sustained-attention driving task implemented in an immersive driving simulator. (a) The driving simulator was mounted on a motion platform.

ISSN No: 2348-4845
International Journal & Magazine of Engineering, Technology, Management and Research
A Peer Reviewed Open Access International Journal

The VR scene simulates nighttime cruising at a speed of 100 km/hr on a four-lane highway without other traffic. (b) The event-related lane-departure paradigm. Deviation onset: the time interval when the car starts to drift to the right or left of the cruising lane. (c) Response onset: the time interval when subjects use the steering wheel. (d) Response offset: the time interval when the car returns to the original lane.

Additionally, the server also received the data via RS-232 compatible serial port from the client which ran the VR program and recorded the behavioral response. This data stream with an 8-bit digital resolution including the vehicle trajectory (0–240), deviation onset (251/252 for left and right side of the deviation), response onset (253), and response offset (254), was synchronized with the EEG data for further event-related analysis.

C. Experimental Paradigm

The event- related land -departure paradigm [43](Fig. 5) was implemented in the VR driving simulator. This paradigm at-tempted to replicate a nonideal road surface to make the car randomly drift out of the cruising lane (deviation onset) at a deviation speed of 5 km/hr toward the left or right side. When encountering each lane-departure event [Fig. 5(b)], which occurred approximately every 8–12 s, the subject was instructed to steer the car (response onset) back to the center of the original lane (response offset) immediately [Fig. 5(c)].

During a 90 min experiment, the total number of trials available from each subject was next, the subject's vigilance level in each trial was quantified using the reaction time (RT, the duration between the deviation onset and the response onset). As is assumed, al-though the subject was alert during the experiment, their RT was fast, whereas a slow RT accompanied the occurrence of drowsiness.

IV. EXPERIMENTAL RESULTS

A. Relationship between RTS and Power Spectra

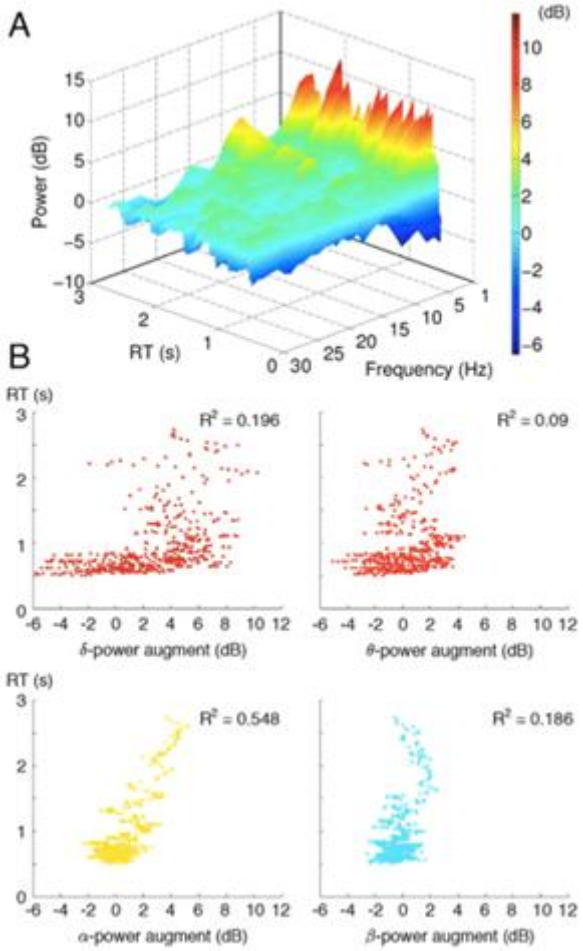

Fig. 6 shows the spectral EEG changes in response to changes in the increase of RT, where denotes the square of Pearson's correlation coefficient. The power spectra of four EEG recordings were averaged and converted into a logarithmic scale in order to form a log power spectrum. Amplitudes of the 2 s prestimulus EEG spectrum were then used to correlate with the following RT. Most studies [15], [44], [45] identified significant increases in the delta and theta activities, which were strongly correlated with the deterioration of task performance. However, according to our results, the changes of delta ( ) and Fig. 6. (a) RT-sorted spectral changes across 1–30 Hz. (a) Delta-power (left-upper), theta-power (right-upper), alpha-power (left-lower), and beta-power (right-lower) augments as the RT changes.

ISSN No: 2348-4845
International Journal & Magazine of Engineering, Technology, Management and Research
A Peer Reviewed Open Access International Journal

theta ( ) powers were not linearly correlated with the RTs. The eye movements may have profoundly affected the EEG power bands, especially for the delta activity. The alpha power and the (theta+alpha)/beta and alpha/beta power ratios are commonly proposed as meaningful indices of poor performance, fatigue, and arousal [45]–[48]. Consistent with the results of these investigations, this study (Fig. 6) suggests that monotonic increases in power spectrum, as evident in the alpha range ( ), can be used as a potential indicator of the vigilance state.

B. System Performance

The feasibility of predicting drivers' vigilance level based on spectral EEG patterns was examined by comparing the prediction performance of using either delta power ( ), theta power ( ), alpha power ( ), beta power ( ), the concatenation of four bands , or the power spectra of 1–30 Hz as the feature vectors for training a SVR. The prediction performances of SVR using linear, polynomial, radial basis function (RBF), and sigmoid kernel functions were also compared. Regarding the performance validation (Table II), two-fold cross-validation was performed and run 100 times to yield the average results. Restated, half of data (257 samples) were randomly selected as the training data, and the remaining data (257 samples) were selected as the validation data.

The performance was evaluated by the root mean square error (RMSE) and squared between the recorded RT and the predicted RT. The number of trained support vectors was also reported. Each cell represents the of the measures. In terms to using the EEG features, SVR with a RBF kernel trained by the alpha power yields the lowest RMSE () and the highest (), compared to the delta (RMSE::), theta (RMSE::), and beta powers (RMSE:). When using the concatenation of four band powers, RMSE decreased to and the increased to Moreover, the RMSE decreases to and the increased to when RBF-SVR used the spectral power of 1–30 Hz as the feature vectors. The number of support vectors tended to de-crease if the number of features increased.

Additionally, SVR with a RBF kernel, which was trained by the spectral power of 1–30 Hz, used the least number of support vectors (36% of the data), compared to other methods (50–70% of the data). The highlighted cells indicate the optimum results among all of the combinations of learning algorithms and spectral features. Overall, SVR using a RBF kernel yields a higher prediction ac-curacy than that using linear, polynomial, and sigmoid kernel functions. According to the safety distance between vehicles re-ported by the Road Safety Authority [49], a minimum reaction distance of 20 m is recommended when driving at a speed of 100 km/h.

Notably, the RMSEs obtained by the proposed system ranges from 124 ms to 481 ms (about 3–13 m at a 100 km/hr car speed), which does not violate the recommended reaction distance. Additionally, the best performance of this study is com-parable with our previous result (RMSE: 130 ms) [13] in which the drowsiness detection system used the EEG signals acquired by the NeuroScan. Fig. 7 further compares the prediction result of SVR using different kernel functions, where SVR was trained by using the spectral powers of 1–30 Hz. The black trace is the recorded RT sorted from fast to slow, and the color traces are RT predicted by different methods. The black bars denote the absolute differences between the recorded RT and the predicted RT. This finding clearly indicates that SVR with a RBF kernel had a higher prediction accuracy than that of other methods, especially for the prediction of fast and slow RTs.

Additionally, the uniform distribution of prediction errors across the entire spectrum of RT revealed how the RBF-based SVR provided the de-sired robustness for forecasting human behaviors. In our previous study [50], polymer foam-based sensors were used in the dry EEG system to record subject's forehead EEG signal. Although RMSE of the prediction result was comparable with those obtained in this study (versus), the artificial noises caused by eye blinking and movement were observed pervasively in the forehead

ISSN No: 2348-4845
International Journal & Magazine of Engineering, Technology, Management and Research
A Peer Reviewed Open Access International Journal

EEG, possibly decreasing the system performance [51].

TABLE II
PREDICTION RESULTS OF REACTION TIMES USING SVR WITH DIFFERENT KERNEL FUNCTIONS

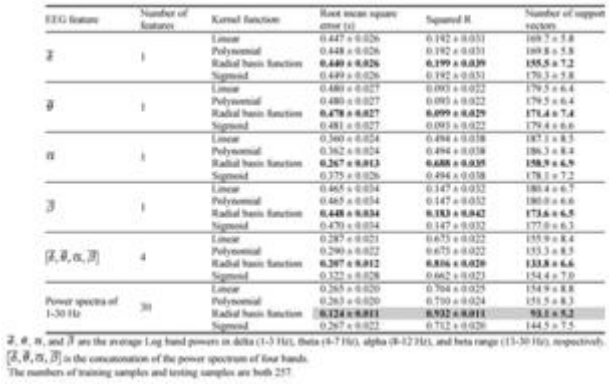

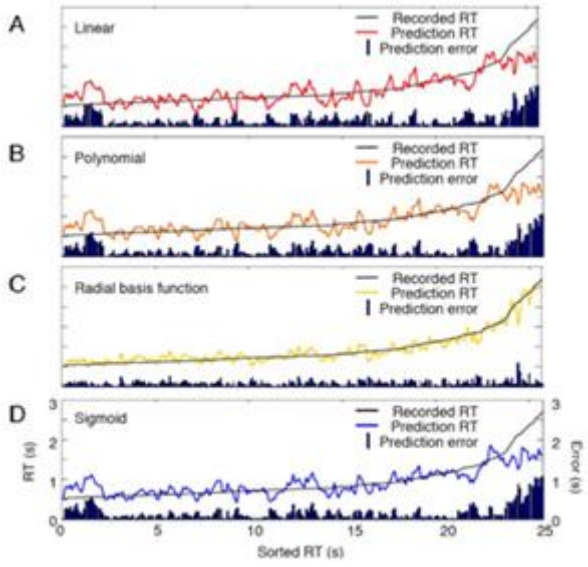

Fig. 7. RTs predicted by support vector regression using (a) linear, (b) polynomial, (c) RBF, and (d) sigmoid kernels. Black and color traces indicate the recorded RT and the prediction RT, respectively. Black bars denote the prediction errors (i.e., absolute difference between recorded RTs and predicted RTs).

Fig. 8 compares the system performance using SVRs with other state-of-art regression methods [52], including linear regression (Linear:), ridge regression (Ridger:), least absolute shrinkage and selection operator (Lassor:), kernel smoother (Ksmoothr:), Pseudo-inverse regression (Pinvr:), partial least squares regression (Plsr: nearest-neighbor regression (knnr:). Analysis results indicated that RMSE obtained by RBF-SVR is better than those using other methods.

C. Real-Time Vigilance Prediction

Above results suggest that the EEG -based system using the RBF-based SVR is a highly promising means of predicting the driver's vigilance level. An attempt was also made to verify the feasibility of the proposed system by further implementing the SVR model in Java language as an Android application, in which the parameters of the implemented model (including slack parameter of SVR, gamma value of RBF kernel, and sup-port vectors of the obtained model) were trained using Matlab software.

Fig. 9 shows a temporal relationship between the vigilance levels predicted by the proposed system and driver's behavior in response to regular traffic events or emergencies when the participant performed the lane-departure driving task for approximately 70 min. The predicted results were converted into eight degrees of vigilance level every 2 s according to Table III which shows the conversion of predicted RT into vigilance level. At the beginning of the experiment, the relatively alert state (bluish bars) was predicted and lasted continuously for several minutes.

TABLE III
INTERPRETATION OF THE VIGILANCE DEGREE PREDICTED BY THE PROPOSED SYSTEM

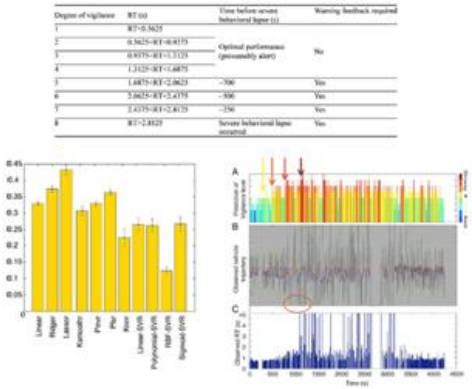

ISSN No: 2348-4845
International Journal & Magazine of Engineering, Technology, Management and Research
A Peer Reviewed Open Access International Journal

Fig. 8. Prediction results compared to state-of-art regression methods, including linear regression (Linear), ridge regression (Ridger), least absolute shrinkage and selection operator (Lassor), kernel smoother (Ksmoothr), Pseudo-inverse regression (Pinvr), partial least squares regression (Plsr), -nearest-neighbor regression (knnr), SVR with a linear kernel (linear- SVR), SVR with a polynomial kernel (polynomial -SVR), SVR with a RBF kernel (RBF-SVR), and SVR with a sigmoid kernel (Sigmoid-SVR). Fig. 9. Temporal changes in (a) the vigilance level predicted by the proposed system, (b) the vehicle trajectory, and (c) the RT observed during a 70 min experiment.

In terms to the behavioral performance, the vehicle trajectory [Fig. 9(b)] and RT [Fig. 9(c)] in response to the unexpected departure indicated that the subject could correct the lane departure promptly (i.e.,). However, the severe behavioral lapse (i.e., the vehicle hit the right or left roadside) appeared at . To avoid car accidents, delivering a warning signal to alert the driver to the danger is necessary if "low vigilance related to severe behavioral lapse" is detected. As shown in Fig. 9, the 5th- (yellow bar), 6th- (orange bar), 7th- (red bar), and 8th-(brown bar) degree of vigilance detected by the proposed system first appeared at , , , and , respectively. This observation suggests that delivering a warning feedback no later than the appearance of 7th-degree of the vigilance is highly recommended to alert drivers to the danger of the declining vigilance and prevent behavioral lapses. This relationship between the predicted level of vigilance and behavior is summarized in Table III.

V. CONCLUSION

This study developed a driver vigilance prediction system with a wireless and wearable EEG device, an efficient pre-diction model, and a real -time mobile App to remedy for drowsy driving. Based on the proposed EEG system, a link was established between the fluctuation in the behavioral index of driving performance (i.e., increase in RT) and the changes in the brain activity (i.e., trends in EEG power spectra). Experimental results indicated that the RMSE could minimize to 0.124 ms when the SVR with a RBF kernel was applied as the prediction model. Additionally, this SVR-based prediction model was implemented in real time for the subjects when they performed a sustained-attention driving task. In the future, combining the proposed methods and the warning feedback system might lead to a practical closed -loop system to predict, monitor and rectify behavioral lapses of human operators in attention-critical settings.

REFERENCES

[1] F. Vaca, J. S. Harris, H. G. Garrison, and M. P. McKay, "Drowsy driving," Ann. Emerg. Med., vol. 45, no. 4, pp. 433–434, 2005.

[2] P. P. Caffier, U. Erdmann, and P. Ullsperger, "Experimental evaluation of eye-blink parameters as a drowsiness measure," Eur. J. Appl. Physiol., vol. 89, no. 3, pp. 319–325, 2003.

[3] Q. Ji, Z. Zhu, and P. Lan, "Real-time nonintrusive monitoring and pre-diction of driver fatigue," IEEE Trans. Veh. Technol., vol. 53, no. 4, pp. 1052–1068, Jul. 2004.

[4] J. Horne and L. Reyner, "Vehicle accidents related to sleep: A review," Occupat. Environ. Med., vol. 56, no. 5, pp. 289–294, May 1999.

[5] S. K. L. Lal and A. Craig, "A critical review of the psychophysiology of driver fatigue," Biol. Psychol., vol. 55, no. 3, pp. 173–194, Feb. 2001.

[6] S. Makeig and T.-P. Jung, "Tonic, phasic, and transient EEG correlates of auditory awareness in drowsiness," Cogn. Brain Res., vol. 4, no. 1, pp. 15–25, 1996.

[7] S. K. L. Lal and A. Craig, "Driver fatigue: Electroencephalography and psychological

assessment," Psychophysiol., vol. 39, no. 3, pp. 313–321, 2002.

[8] L. Chin-Teng, C. Che-Jui, L. Bor-Shyh, H. Shao-Hang, C. Chih-Feng, and I. J. Wang, "A real-time wireless brain-computer interface system for drowsiness detection," IEEE Trans. Biomed. Circuits Syst., vol. 4, no. 4, pp. 214–222, Aug. 2010.

[9] C. Guger et al., "How many people are able to control a P300-based brain-computer interface (BCI)?," Neurosci. Lett., vol. 462, no. 1, pp. 94–98, Oct. 2009.

[10] M. A. Schier, "Changes in EEG alpha power during simulated driving: A demonstration," Internat. J. Psychophysiol., vol. 37, no. 2, pp. 155–162, Aug. 2000.

[11] C. Papadelis et al., "Monitoring sleepiness with on-board electrophys-iological recordings for preventing sleep-deprived traffic accidents," Clin. Neurophysiol., vol. 118, no. 9, pp. 1906–1922, Sep. 2007.

[12] S. Makeig, T.-P. Jung, and T. Sejnowski, "Awareness during drowsi-ness: Dynamics and electrophysiological correlates," Can. J. Exp. Psy-chol., vol. 54, no. 4, pp. 266–273, 2000.

[13] F.-C. Lin, L.-W. Ko, C.-H. Chuang, T.-P. Su, and C.-T. Lin, "Gener-alized EEG-based drowsiness prediction system by using a self-orga-nizing neural fuzzy system," IEEE Trans. Circuits Syst. I, Reg. Papers, vol. 59, no. 9, pp. 2044–2055, Sep. 2012.

[14] C.-T. Lin et al., "Tonic and phasic EEG and behavioral changes in-duced by arousing feedback," NeuroImage, vol. 52, no. 2, pp. 633–642, Aug. 2010.

[15] C.-T. Lin, C.-H. Chuang, Y.-K. Wang, S.-F. Tsai, T.-C. Chiu, and L.-W. Ko, "Neurocognitive characteristics of the driver: A review on drowsi-ness, distraction, navigation, and motion sickness," J. Neurosci. Neu-roengin., vol. 1, no. 1, pp. 61–81, Jun. 2012.

[16] C.-T. Lin, I.-F. Chung, L.-W. Ko, Y.-C. Chen, S.-F. Liang, and J.-R. Duann, "EEG-based assessment of driver cognitive responses in a dy-namic virtual-reality driving environment," IEEE Trans. Biomed. Eng., vol. 54, no. 7, pp. 1349–1352, Jul. 2007.

[17] C. H. Chuang, L. W. Ko, Y. P. Lin, T. P. Jung, and C. T. Lin, "Independent component ensemble of EEG for brain-computer interface," IEEE Trans. Neural Syst. Rehabil. Eng., vol. 22, no. 2, pp. 230–238, Mar. 2014.

[18] T. C. Ferree, P. Luu, G. S. Russell, and D. M. Tucker, "Scalp electrode impedance, infection risk, and EEG data quality," Clin. Neurophysiol., vol. 112, no. 3, pp. 536–544, Mar. 2001.

[19] X. Jiawei, R. F. Yazicioglu, B. Grundlehner, P. Harpe, K. A. Makinwa, and C. Van Hoof, "A 160 muW 8-channel active electrode system for EEG monitoring," IEEE Trans. Biomed. Circuits Syst., vol. 5, no. 6, pp. 555–567, Dec. 2011.

[20] T. I. Oh et al., "Nanofiber web textile dry electrodes for long-term biopotential recording," IEEE Trans. Biomed. Circuits Syst., vol. 7, no. 2, pp. 204–11, Apr. 2013.

[21] G. Gargiulo et al., "A new EEG recording system for passive dry electrodes," Clin. Neurophysiol., vol. 121, no. 5, pp. 686–693, May 2010.

[22] T. O. Zander et al., "A dry EEG-system for scientific research and brain-computer interfaces," Front Neurosci., vol. 5, no. 53, pp. 1–10, 2011.

[23] Brainwave EEG Signal, NeuroSky, Dec. 5, 2009 [Online]. Available: http://www.neurosky.com

ISSN No: 2348-4845
International Journal & Magazine of Engineering, Technology, Management and Research
A Peer Reviewed Open Access International Journal

[24] C. Grozea, C. D. Voinescu, and S. Fazli, "Bristle-sensors—low-cost flexible passive dry EEG electrodes for neurofeedback and BCI applications," J. Neural. Eng., vol. 8, no. 2, pp. 1–8, Apr. 2011.

[25] C.-T. Lin, L.-D. Liao, Y.-H. Liu, I.-J. Wang, B.-S. Lin, and J.-Y. Chang, "Novel dry polymer foam electrodes for long-term EEG mea-surement," IEEE Trans. Biomed. Eng., vol. 58, no. 5, pp. 1200–1207, 2011.

[26] L.-D. Liao et al., "Biosensor technologies for augmented brain-computer interfaces in the next decades," Proc. IEEE, vol. 100, pp. 1553–1566, May 2012, Special Centennial Issue.

[27] L.-D. Liao et al., "Gaming control using a wearable and wireless EEG-based brain-computer interface device with novel dry foam-based sen-sors," J. Neuroeng. Rehabil., vol. 9, no. 5, pp. 1–11, Jan. 2012.

[28] L.-D. Liao, I.-J. Wang, S.-F. Chen, J.-Y. Chang, and C.-T. Lin, "De-sign, fabrication and experimental validation of a novel dry-contact sensor for measuring electroencephalography signals without skin preparation," Sensors, vol. 11, no. 6, pp. 5819–5834, 2011.

[29] L. D. Liao et al., "A novel 16-channel wireless system for electroencephalography measurements with dry spring-loaded sensors," IEEE Trans. Instrum. Meas., vol. 63, no. 6, pp. 1545–1555, Jun. 2014.

[30] A. J. Smola and B. Schölkopf, "A tutorial on support vector regres-sion," Statist. Comput., vol. 14, no. 3, pp. 199–222, 2004.

[31] R.-S. Huang, T.-P. Jung, and S. Makeig, "Tonic changes in EEG power spectra during simulated driving," Lecture Notes Comput. Sci., vol. 5638 LNAI, pp. 394–403, 2009.

[32] C.-T. Lin, I. F. Chung, L.-W. Ko, Y.-C. Chen, S.-F. Liang, and J.-R. Duann, "EEG-based assessment of driver cognitive responses in a dynamic virtual-reality driving environment," IEEE Trans. Biomed. Eng., vol. 54, no. 7, pp. 1349–1352, Jul. 2007.

[33] W. Karlen, C. Mattiussi, and D. Floreano, "Sleep and wake classification with ECG and respiratory effort signals," IEEE Trans. Biomed. Circuits Syst., vol. 3, no. 2, pp. 71–78, Apr. 2009.

[34] M. A. Haberman and E. M. Spinelli, "A multichannel EEG acquisition scheme based on single ended amplifiers and digital DRL," IEEE Trans. Biomed. Circuits Syst., vol. 6, no. 6, pp. 614–618, Dec. 2012.

[35] D. Neamen, Microelectronics Circuit Analysis and Design, 3rd ed. New York, NY, USA: McGraw-Hill, 2007.

[36] S. Makeig and M. Inlow, "Lapses in alertness: Coherence of fluctuations in performance and EEG spectrum," Electroencephalogr. Clin. Neurophysiol., vol. 86, no. 1, pp. 23–35, Jan. 1993.

[37] A. Alenezi, S. A. Moses, and T. B. Trafalis, "Real-time prediction of order flowtimes using support vector regression," Comput. Operat. Res., vol. 35, no. 11, pp. 3489–3503, 2008.

[38] U. Thissen, M. Pepers, B. Üstün, W. J. Melssen, and L. M. C. Buydens, "Comparing support vector machines to PLS for spectral regression applications," Chemometr. Intell. Lab. Syst., vol. 73, no. 2, pp. 169–179, 2004.

[39] C.-C. Chang and C.-J. Lin, "LIBSVM: A Library for support vector machines," ACM Trans. Intell. Syst. Technol., vol. 2, no. 3, pp. 1–27, Apr. 2011.